Neuro-Oncology 14(5):574–583, 2012.
doi:10.1093/neuonc/nos061
Advance Access publication March 29, 2012

Global gene expression profiling confirms the molecular fidelity of primary tumor-based orthotopic xenograft mouse models of medulloblastoma

Xiumei Zhao, Zhigang Liu, Litian Yu, Yujing Zhang, Patricia Baxter, Horatiu Voicu, Sivashankarappa Gurusiddappa, Joseph Luan, Jack M. Su, Hon-chiu Eastwood Leung, and Xiao-Nan Li

Laboratory of Molecular Neuro-Oncology, Texas Children's Cancer Center, Houston, Texas (X.Z., Z.L., L.Y., Y.Z., X.-N.L.); Texas Children's Cancer Center, Houston, Texas (X.Z., Z.L., L.Y., Y.Z., P.B., H.V., S.G., J.L., J.M.S., H.-C.E.L., X.-N.L.); Department of Molecular and Cellular Biology, Texas Children's Hospital, Baylor College of Medicine, Houston, Texas (H.-C.E.L.); Dan L. Duncan Cancer Center, Houston, Texas (H.-C.E.L., X.-N.L.)

We previously showed that primary tumor-based orthotopic xenograft mouse models of medulloblastoma replicated the histopathological phenotypes of patients' original tumors. Here, we performed global gene expression profiling of 11 patient-specific xenograft models to further determine whether the xenograft tumors were molecularly accurate during serial subtransplantations in mouse brains and whether they represented all the molecular subtypes of medulloblastoma that were recently described. Analysis of the transcriptomes of 9 pairs of matched passage I xenografts and patients' tumors revealed high correlation coefficients ($r^2 > 0.95$ in 5 models, > 0.9 in 3 models, and > 0.85 in 1 model) and only identified 69 genes in which expressions were altered (FDR = 0.0023). Subsequent pair-wise comparisons between passage I, III, and V xenografts from the 11 models further showed that no dramatic alterations were introduced ($r^2 > 0.9$ in 8 models and > 0.8 in 3 models). The genetic abnormalities of each model were then identified through comparison with control RNAs from 5 normal cerebella and 2 fetal brains. Hierarchical clustering using 3 previously published molecular signatures showed that our models span the whole spectrum of molecular subtypes, including SHH ($n = 2$), WNT ($n = 2$), and the most recently identified group C ($n = 4$) and group D ($n = 3$). In conclusion, we demonstrated that the 11 orthotopic medulloblastoma xenograft models were molecularly faithful to the primary tumors, and our comprehensive collection of molecularly distinct animal models should serve as a valuable resource for the development of new targeted therapies for medulloblastoma.

Keywords: cancer stem cell, glioma, medulloblastoma, orthotopic xenograft model.

Medulloblastoma is the most common malignant brain tumor that occurs in children. Despite an aggressive combination of surgery, radiation, and chemotherapy, medulloblastoma remains incurable in a significant proportion of patients.[1–5] Even among the survivors, many patients are left with long-term neurological and endocrinal sequela. Clinically relevant and molecularly accurate animal models that replicate the biology of this malignant tumor are urgently needed to understand tumor biology and to develop new targeted therapies that are more effective and less toxic.[6]

Compared with traditional cell line–based xenograft mouse models, direct injection of fresh surgical specimens into anatomically matched locations in immunodeficient mice has been shown to better recapitulate the cellular and clinical phenotypes of multiple human cancers.[6,7] For brain tumors, however, orthotopic injection into mouse brains, particularly into the cerebellum where

Received June 15, 2011; accepted January 30, 2012.

Present affiliations: *First Affiliated Hospital, Harbin Medical University, Harbin, PR China (X.Z.)*
Corresponding Author: Xiao-Nan Li, MD, PhD, Laboratory of Molecular Neuro-Oncology, Texas Children's Cancer Center, Texas Children's Hospital, 6621 Fannin St., MC 3–3320, Houston, TX 77030 (xiaonan@bcm.tmc.edu).

medulloblastomas originate, remains a surgically challenging procedure. Using an optimized surgical technique,[8] we recently established a relatively large panel of orthotopic xenograft mouse models of malignant pediatric brain tumors from fresh tumors of patients.[9,10] Histopathological examination showed that the intracerebellar xenografts of medulloblastoma exhibited very similar histology and immunohistochemical phenotypes of patients' original tumors and maintained the invasive/metastatic features even during serial subtransplantations in vivo in mouse brains. We also demonstrated that the xenograft tumor cells can be cryopreserved for long-term preservation of tumorigenicity.[9]

There are still concerns about the molecular fidelity of these xenograft mouse models. This is because the tumor microenvironment can critically affect biological behaviors of xenograft tumors.[11] Despite histological similarities between the human and the mouse cerebellum, their microenvironmental support for medulloblastoma is not identical. The subtle differences between human and mouse cerebella may have a significant impact on the survival and biology of the heterotransplanted medulloblastoma cells. In addition, patients' tumor tissues have to go through a series of mechanical and/or enzymatic dissociation process before being surgically implanted. It is therefore possible that the selective pressure from the tissue-processing procedures, the adaptive changes to the new habitat, and the progressive alterations of the tumor cells may favor the growth of a selective subpopulation of tumor cells, potentially causing significant molecular drift from that of patients' original tumors. This possibility, however, has not been rigorously examined in large panels of patient-derived orthotopic xenograft mouse models, although gene expression profiling in a series of subcutaneous xenograft models of pediatric cancers, which were mostly derived from cell lines, showed that those xenografts closely resemble their tumor types of origin.[12] Because small-molecule inhibitors that selectively target aberrantly activated cell signaling pathways in medulloblastoma could have significant use in the future management of this disease,[13,14] it is important to determine whether and to what extent the gene expression signatures of patients' tumors are preserved in the orthotopic xenograft tumors. In addition, given the rapid advancements of molecular subclassifications of medulloblastoma,[15–21] it is also highly desirable to have a model system in which all the major molecular subtypes are well represented so that new targeted therapies can be tested in genetically appropriate animal models.

Here, we describe our examination of molecular fidelity of 11 primary tumor-based orthotopic xenograft mouse models of medulloblastoma. To test our hypothesis that primary tumor-based orthotopic xenograft mouse models would faithfully replicate the genetic abnormalities of patients' original tumors even during serial in vivo subtransplantations, we performed whole genome gene expression to determine whether xenograft tumors replicate the molecular characteristics of their originating human tumors and whether serial in vivo subtransplantations introduce additional changes in gene expression. Because one of the major applications of an animal model system is to conduct preclinical drug screenings of molecular-targeted therapies, we also analyzed the xenograft transcriptomes to determine whether or not our models can be partitioned into the molecular subgroups that have been identified in medulloblastomas[15–18] and to identify activated genes/signaling pathways in these models so that they can be used for rationally designed preclinical drug screenings.

Materials and Methods

Primary Tumor-Based Orthotopic Xenograft Models and Patients' Medulloblastoma

We studied a total of 11 primary tumor-based orthotopic xenograft mouse models that have been subtransplanted in vivo in mouse brains for at least 3 times (Table 1). Histopathological characterization of 8 models has been described previously.[9] These models were established from fresh surgical tissues from 21 children who underwent craniotomy at Texas Children's Hospital. The overall tumor take rate was 52.3% (Supplementary Table S1). The tumor tissues were

Table 1. Summary of histopathological features of the 11 medulloblastomas

Model ID	Age	Gender	Pathological Subtype	Northcott Group	Reference
ICb-1078MB	11 y 9 mo	Male	Anaplastic	D	new
ICb-1140MB	6 y	Male	Anaplastic	WNT	new
ICb-1299MB	2 y 9 mo	Female	Anaplastic	D	9
ICb-1494MB	5 y 2 mo	Female	Anaplastic	C	9
ICb-1595MB	15 mo	Female	Anaplastic	C	new
ICb-984MB	7 y 10 mo	Female	Anaplastic	SHH	9
ICb-1192MB	12 y 5 mo	Male	Classic	WNT	9
ICb-1487MB	6 y 11 mo	Male	Classic	D	new
ICb-1572MB	14 y 9 mo	Male	Large cell	C	9
ICb-1197MB	5 y	Male	Desmoplastic	C	9
ICb-1338MB	0 y 6 mo	Male	Desmoplastic	SHH	9

obtained through informed consent in accordance with institutional review board–approved protocols, and all animal experiments were conducted using an Institutional Animal Care and Use Committee–approved protocol.[9,10] In brief, the Rag2 SCID mice were bred and housed in a specific pathogen-free animal facility at Texas Children's Hospital. Surgical transplantation of tumor cells into each mouse's cerebellum, usually completed within 60 min after tumor removal, was performed as described previously.[9] Both male and female mice, aged 6–8 weeks, were anesthetized with sodium pentobarbital (50 mg/kg, intraperitoneal injections). Tumor cells (1×10^5) were suspended in 2 μL of culture medium and injected into the right cerebellum (1 mm to the right of the midline, 1 mm posterior to the lamboidal suture, and 3 mm deep) with use of a 10 μL 26-gauge Hamilton Gastight 1701 syringe needle. The animals were then monitored daily for development of neurological deficits, at which time they were euthanized, and their brains were removed for histopathologic examination and tumor tissue harvest.

Serial Subtransplantations of Xenografts In Vivo in Mouse Brains

Whole brains of donor mice were aseptically removed, coronally cut into halves, and transferred back to the tissue culture laboratory. Tumors were dissected under the microscope, mechanically dissociated into cell suspensions, and then injected into the brains of recipient SCID mice as described above.[9,10]

Whole-Genome Gene Expression Profiling

The genome-wide expression analysis was performed using Illumina's Human-6 v2 Beadchips, which contain more than 48 000 probes, according to the manufacturer's instructions.[10] In brief, total RNA was extracted from original human tumor tissues and intracerebral xenograft tumors with TRIzol reagent (Invitrogen), as described previously.[10,22,23] Normal control human cerebellar RNAs from 5 adults and total RNAs from 2 fetal brains were procured from a commercial source (Clontech Laboratories and Biochain). Total RNA from a warm autopsied cerebellum of an 8-year-old child was also included. RNA quantitation was checked using an ND-1000 spectrophotometer (Nanodrop Technologies). RNA integrity was checked using 6% formaldehyde gel electrophoresis. Half a microgram of total RNAs was used to synthesize biotinylated cRNA using Totalprep RNA amplification kit (Ambion), and 1.5 μg of biotinylated cRNA was applied to the Human-6 v2 Beadchips and processed according to the vendor's instructions (Illumina). The Beadchips were scanned using a Beadstation 500 GX scanner. Background was subtracted, and the spectra were processed using the quantile normalization function in Genomestudio software, version 2009 v1. A total of 6775 genes (detection $P <$ .001 for all samples) were used for the clustering analysis. Data were imported into Bioconductor software and processed for heatmap and hierarchical clustering dendrogram generation. Differential genes were discovered using significant analysis of microarray[24] with various controlled false discovery rate (FDR). Pathway analysis was performed using Metacore software (Genego).

Quantitative Real-Time Polymerase Chain Reaction (qRT-PCR)

Quantitative analysis of differentially expressed genes were performed using qRT-PCR with SYBR green master mix in an ABI 7000 DNA detection system (ABI), as we previously described.[10,22,23] Complementary DNA was synthesized using MuLV reverse transcriptase and random hexamers (Perkin Elmer) in a total volume of 20 μL from 1 μg of total RNA extracted with Trizol reagent (Invitrogen). Primers for PCR amplification were designed to flank more than 1 exon (Supplementary Table S2). Expression levels of selected genes were normalized to the internal standard GAPDH with use of the standard ΔΔCt method. All reactions were performed in duplicate and repeated twice, and the specificities of PCR products were confirmed by analyzing dissociation curves from individual reactions and visualizations on 2% agarose gel.

Results

Comparison of Gene Expression Profiles Between Xenograft Tumors of the First Passage and Their Matched Original Patients' Tumors

To determine whether the xenograft tumors maintained global gene expression characteristics of the corresponding patients' tumors, we used Illumina's gene expression microarrays to compare the gene expression profiles of 9 xenograft tumors from passage I with that of the corresponding patients' tumors, of which tumor RNAs were available. We also included a panel of normal fetal brain ($n = 4$), adult cerebellum ($n = 5$), and childhood cerebellum ($n = 1$) samples that were analyzed simultaneously as the normal controls. The normalized and raw data were deposited in GEO (accession number GSE28192; www.ncbi.nlm.nih.gov/geo/). From the 42 620 elements on the microarray, we identified 6775 genes that have the detection $P <$ .001 in all 94 arrays. Using these genes to calculate correlation coefficients, we found a strong positive correlation ($P <$ .0001) between the profiles of patients' tumors and the corresponding xenograft tumors from passage I (mean ± standard deviation (SD), $r^2 = 0.956 \pm 0.018$; $r^2 > 0.95$ in 7 models; > 0.9 and > 0.85 in the remaining 2 models, respectively) (Fig. 1, Supplementary Fig. S1). These results suggest that the overall gene expression profiles of the patients' tumors were well-maintained in the primary passage of xenograft tumors.

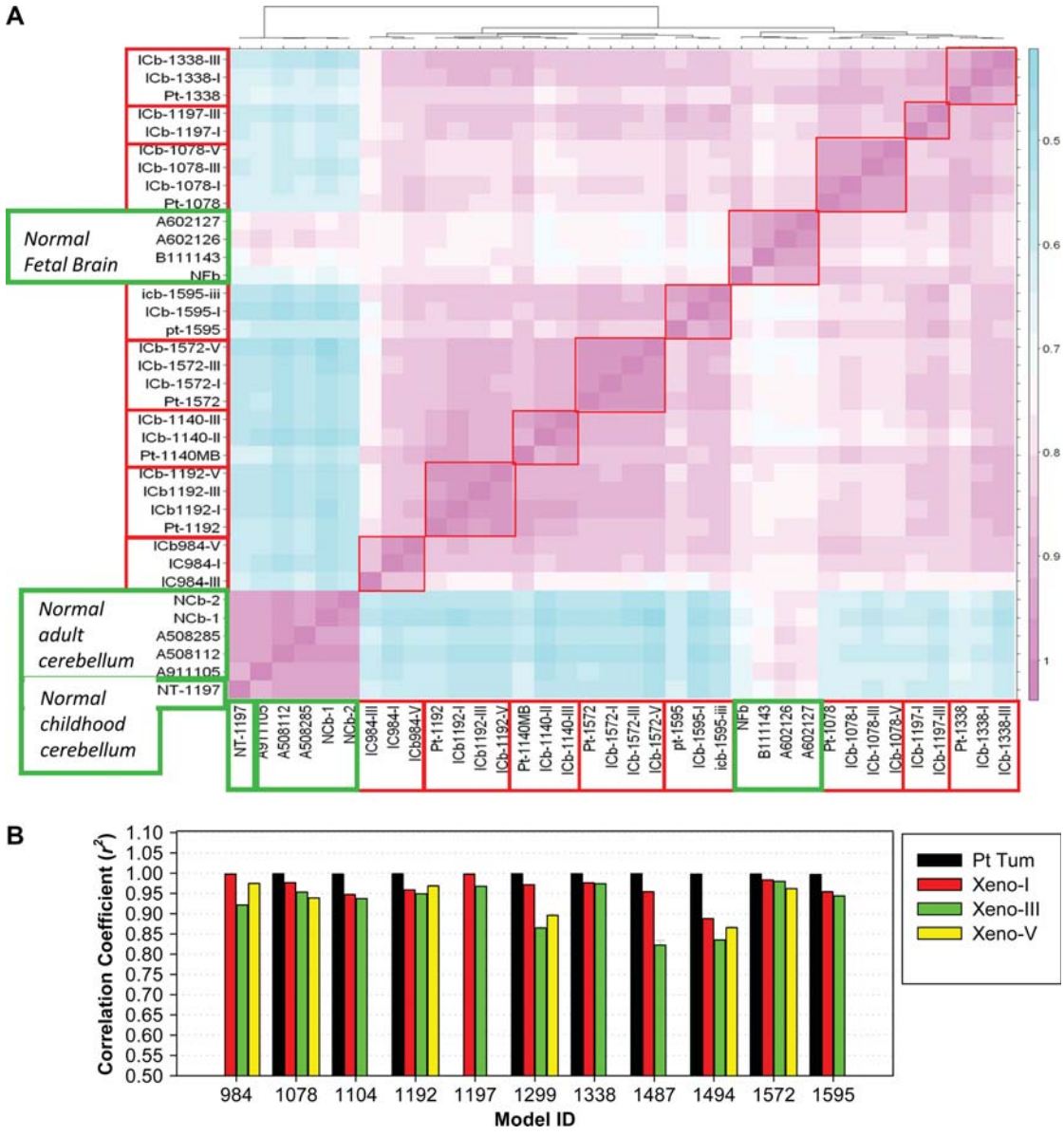

Fig. 1. Summary of correlation coefficients using 6775 genes that have the detection $P < .001$ in all 94 arrays. (A) Hierarchical clustering of overall correlation in the 9 models with high correlation coefficients ($r^2 > 0.9$). The value of r^2 was used as a metric for building the dendrogram. The dendrogram at the top of the figure shows the grouping of the samples. The length of the legs is indicative of the correlation among the samples. The shorter the legs, the closer they are. Patients' tumors (Pt) and intracerebellar (ICb) xenograft tumors during serial subtransplanation from passage I (I) to passage V (V) were compared with normal brain tissue. (B) Graph highlighting the correlation either between xenograft tumors and their corresponding patients' tumors or between serially passaged xenograft tumors (passage III and V) with the passage I xenograft tumors when patients' tumors were not available (case #984 and #1197).

We next compared the gene expression signatures of our medulloblastoma xenografts with the normal human cerebella and the normal fetal brain samples. The profiles of adult cerebellar tissue clustered close to the normal cerebellar RNA obtained from an 8-year-old child, and they both have a low correlation with the fetal brain samples. Compared with low correlation coefficients ($r^2 < 0.6$) between the medulloblastomas (both the patients' tumors and xenografts) and the normal adult and child cerebellar RNAs, higher ($r^2 = 0.7–0.8$) coefficients were found between the fetal brains and medulloblastomas (Fig. 1). These data suggest that the genetic signatures of our xenograft models share more similarity with fetal brains than do the adult cerebella.

Comparison of Gene Expression Profiles of Xenograft Tumors During Serial In Vivo Subtransplantations

Serial subtransplantation is important for the demonstration of sustained tumorigenicity and for the expansion of

usable mouse numbers of the established xenograft models.[9] To determine whether serial in vivo subtransplantations introduced significant changes of gene expression profiles, comparisons were made between xenograft tumors (passage III and V) and their corresponding patients' tumors with the use of the 6775 genes that have the detection $P < .001$ in all 94 arrays. High correlation was observed when the xenograft tumors from passage III ($n = 11$) were compared with the patients' tumors (mean $\pm$ SD, $r^2 = 0.918 \pm 0.051$; $r^2 > 0.95$ in 3 models, $r^2 > 0.9$ in 4 models, and $r^2 > 0.8$ in 2 models). When the passage V xenograft tumors ($n = 4$) were compared with their patients' tumors, similar high correlates were observed ($r^2 > 0.95$ in 2 models, > 0.9 and > 0.85 in 1 model each) (Fig. 1).

Gene Expression and Pathway Analysis for the Transition from Patients' Tumors to Primary Xenograft Tumors and During Serial Subtransplantation In Vivo

To identify genes/signaling pathways that were either lost or activated from the patients' tumors during subtransplantation, differential gene expression profiles from the xenograft tumors (passage I) were compared with the corresponding patients' tumors. At an FDR of 0.0006, we identified 69 genes with fold change 1.8 or more. A total of 59 genes were overexpressed, and 10 genes were downregulated in passage I xenograft tumors. Gene-ontology analysis showed that only 3 pathways were significantly altered ($P < .003$; FDR = 0.05): (1) the transport RAN regulatory pathway, (2) angiotensin signaling pathway via STATs, and (3) p53 signaling pathway (Fig. 2 and Supplementary Fig. S2A).

To identify the genetic changes that were induced during serial subtransplantation in vivo in mouse brains, similar analysis was performed using the FDR (0.01) and fold change (1.8) as filters. A total of 30 genes (FDR = 0.023) were identified between passage III and passage I xenografts (30 upregulated and 0 downregulated). Seven pathways were found to be altered when the differential genes were fed into pathway analysis (Supplementary Fig. S2B). These pathways included lipid metabolism; cAMP signaling; EDG1, EDG3, EDG5 signaling pathways; and blood coagulation pathways.

Comparison between passage III and V did not show any significant differential genes (FDR = 0.023), although lowering the FDR stringency to 0.03 revealed BCKDHA (fold change = 0.48) as the only significant differential gene. Combined, these results suggest that the major genetic changes occurred during the transition from the patient to the mouse brain, and the gene expression profiles of xenograft tumors during serial subtransplantations were maintained relatively faithfully.

Identification of Xenograft Models Representing Different Molecular Subtypes of Medulloblastoma

Recent studies using genomic analysis suggest that the histological entity of medulloblastoma is composed of 4–5 molecular variants.[15–17] Because the 4–5 subtypes of medulloblastoma are demographically, clinically, transcriptionally, and genetically distinct, they may need to be targeted individually. It will be of prime

A

Transitions	Differentially Expressed Genes	FDR
Patient to P-I xenograft	69	0.0006
P-I to P-III xenograft	30	0.023
P-III to P-V xenograft	1	0.03

B

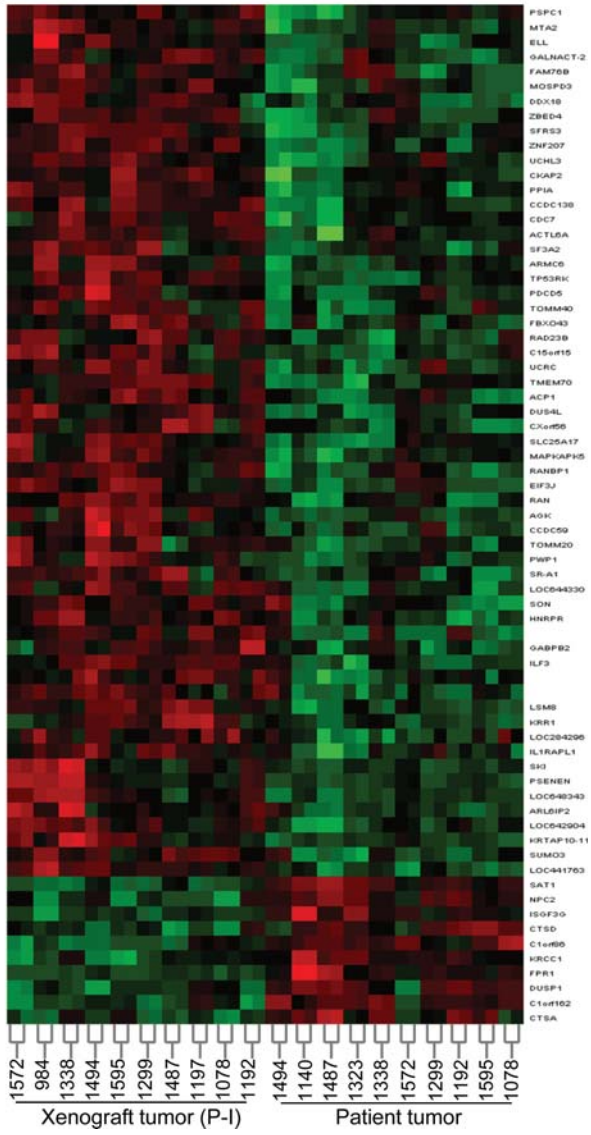

Fig. 2. Gene expression and pathway analysis of 11 medulloblastomas during transition from patients to growth in SCID mice. (A) The list of the numbers of differentially expressed genes from patients' tumors (Patient) to passage I (P-I) xenograft, and during serial subtransplantations up to passage V (P-V)xenograft tumors. (B) Hierarchical clustering of the 69 differentially expressed genes during transition from the patient to passage I xenograft at the false discovery rate (FDR) of 0.0006.

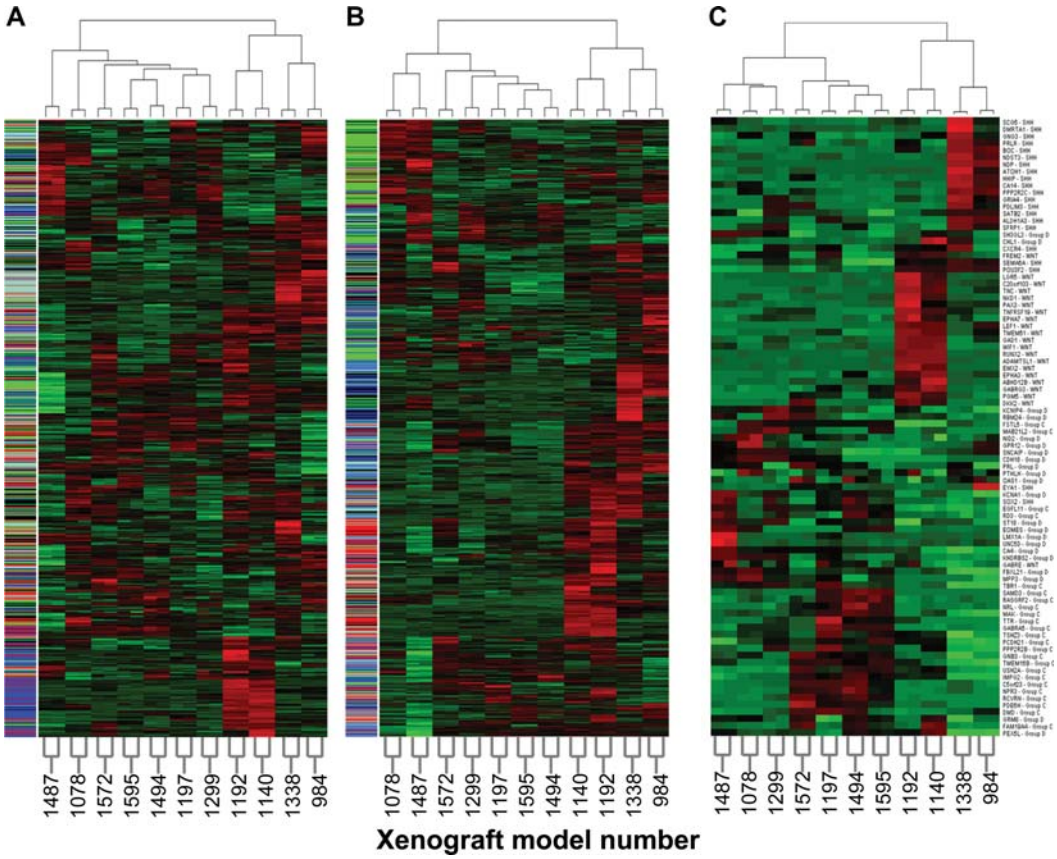

Fig. 3. Hierarchical clustering showing the classification of 11 xenograft models (passage III) using previously reported gene signatures of medulloblastomas. (A) Clustering using 1500 most significant genes from Thompson et al. (2006) study.[15] Color legend: Red (Group A), Blue (Group B), Green (Group C), Aquamarine (Group D), Black (Group E). (B) Clustering using 1500 most significant genes from Kool et al. (2008) study.[16] Color legend: Red (Group A), Blue (Group B), Green (Group C), Aquamarine (Group D), Black (Group E). (C) Classification using the genes provided in the supplemental material from the Northcott et al. (2010) study.[17] All 100 genes provided in the supplemental material were used, and 88 genes from our Illumina platform were successfully used to discriminate between the 4 types of medulloblastomas.

importance to determine whether the animal models in our laboratory represented different classes of medulloblastoma. To examine whether previously reported subtypes are represented in our panel of xenograft models, we used the gene expression profiles from passage III of our xenograft tumors to subgroup them according to the genetic signatures that have been described previously.

Early analysis of gene expression profiles by Thompson et al. (2006) categorized medulloblastomas into 5 distinct groups: A–E.[15] Each tumor subgroup displays a unique gene expression signature of 400–800 transcripts that are significantly upregulated or downregulated. From these transcripts, we selected the 300 most significant genes from each group (for a total of 1500 genes) and clustered our models. As shown in Fig. 3A, we only observed a good discrimination of group B (WNT), although tumors of group A also displayed a tendency to cluster together.

A subsequent study by Kool et al. (2008) identified 5 medulloblastoma subtypes through integrated genomic analysis.[16] In addition to the WNT (cluster A) and SHH signaling (cluster B) subtypes, the remaining 3 subtypes were closely related. They fell apart on the basis of expression of a series of neuronal differentiation genes in cluster C and D and expression of retinal differentiation genes in cluster D and E. Using the 1500 overexpressed genes in Kool's set, we were able to achieve good discrimination and place our models into cluster A (WNT), cluster B (SHH), and cluster C. We were not, however, able to satisfactorily subclassify our models into the clusters D or E (Fig. 3B).

In the most recent study, Northcott et al. (2010) found 1450 high-standard deviation genes that can discriminate between 4 subgroups of medulloblastoma.[17] For classification of our models, all 100 genes provided in the supplemental material were used. The fluorescence intensities from the Illumina chips were normalized using the quantile normalization algorithm, and then, for each gene, the intensities were transformed into standard scores. Using genes that have large standard deviations, we were successful in segregating the 11 models into 4 groups (Fig. 3C). Because the use of 4 single genes were shown to be able to reliably and uniquely classify formalin-fixed medulloblastomas, we applied these 4 genes (DKK1 [WNT], SFRP1 [SHH],

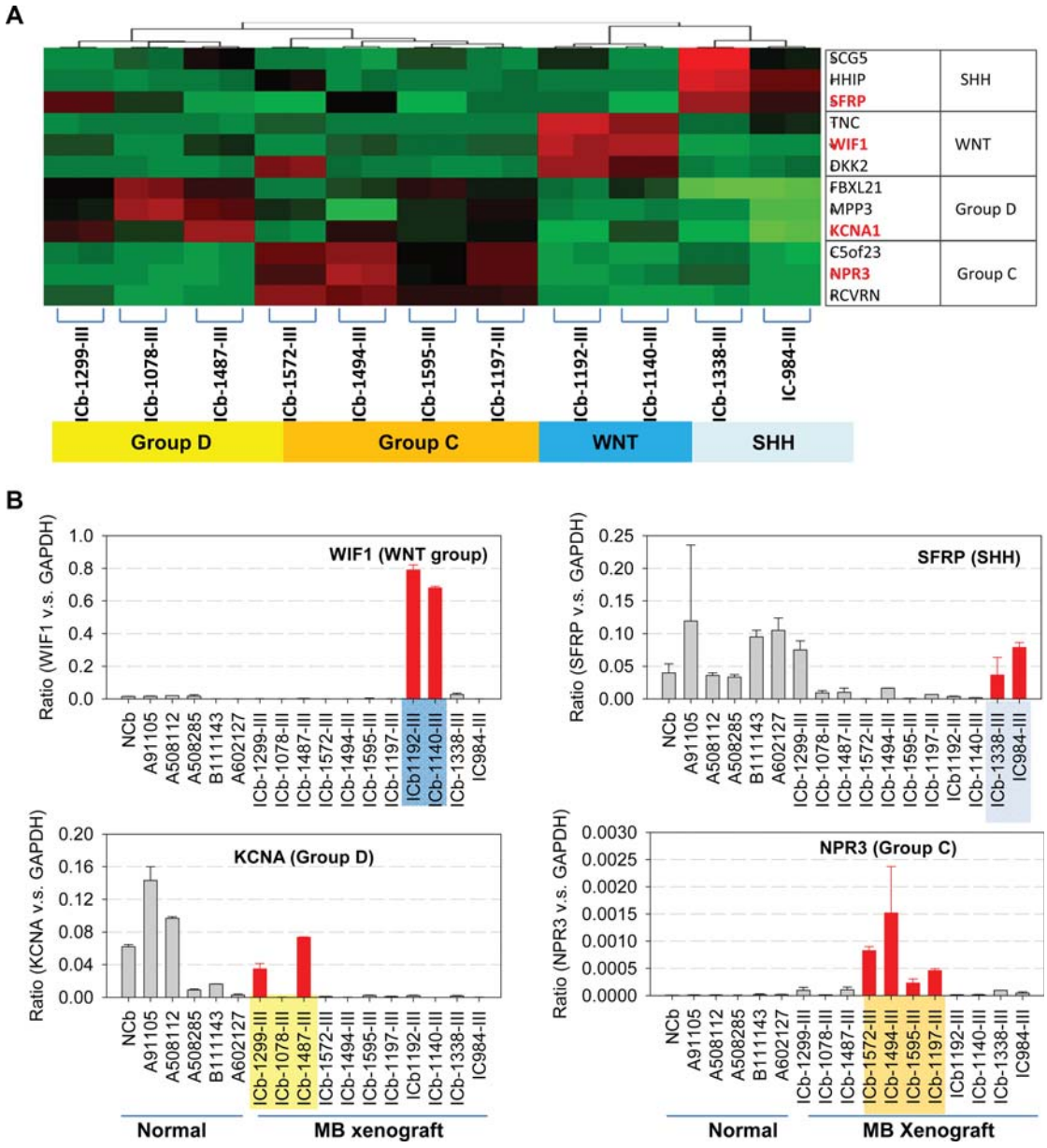

Fig. 4. Molecular subclassification of the 11 xenograft models using the genetic identifiers identified by the Northcott et al. study. (A) Clustering of the 11 xenograft models at passage III with the identified classifiers from gene expression profiling results. For each sample, results from the duplicated array hybridization were presented. Genes highlighted in red were selected for qRT-PCR validation. (B) Validation of differentially expressed subclassifiers with quantitative RT-PCR. Total RNAs from 4 adult cerebella (NCb, A91105, A508112, and A508285) and 2 fetal brains (B111143 and A602127) were included.

NPR3 [group C], and KCNA1 [group D]), together with 2 additional genes from each group that exhibited similar expression patterns to cluster our models using passage III xenograft tumors as representatives. As shown in Fig. 4A, we have 2 models each for WNT and SHH groups, 4 models in group C, and 3 models in group D. To further determine whether this subclassification held true for patients' tumors, we analyzed all the samples using the same molecular classifiers. Except ICb-1299MB passage I that was subclassified into group C and the patients' tumor and passage III xenograft that fell into group D, the patients' tumors and their corresponding xenografts from the remaining models were subclassified into the sample molecular groups (Supplementary Fig. S3). In summary, the panel of orthotopic xenograft models in our laboratory represents the full spectrum of different subtypes of medulloblastoma.

Validation of Differentially Expressed Genes

To validate the results obtained from gene expression profiling, mRNA expression levels of 4 classifiers

identified by Northcott et al. (SFRP [SHH group], WIF1 [WNT group], NPR3 [group C], and KCNA [group D]) [17] were examined using qRT-PCR in the 11 xenograft models (passage III) using total RNAs from 4 normal adult cerebellum and 2 fetal brains as references. Although the expression levels of these 4 genes in the normal adult cerebella and the fetal brains varied, the patterns of their mRNA expression in the xenograft tumors nearly mirrored those found in the gene expression profiling. Over-expression of SFRP was found in only 2 SHH models (ICb-1338MB and ICb-984MB), WIF1 in the 2 WNT models (ICb-1192MB and ICb-1140MB), KCNA in group D tumors (ICb-1078MB and ICb-1487MB), and NPR3 in group C tumors (ICb-1572Mb, ICb-1494MB, ICb-1595MB and ICb-1197MB) (Fig. 4B).

Identification of Potential Therapeutic Markers

One of the major objectives of developing animal models for human cancer is to test new therapies. To identify signaling pathways that are deregulated in these models, we included a panel of normal fetal brain ($n = 4$), adult cerebellum ($n = 5$), and childhood cerebellum ($n = 1$) samples and analyzed them simultaneously with normal controls. The normalized and raw data have been deposited in GEO (accession number GSE28192; www.ncbi.nlm.nih.gov/geo/). To identify uniquely expressed genes or activated signaling pathways that can be therapeutic targets and to facilitate the use of our model system, we released the entire gene expression data set to enable other investigators to develop their own optimized queries and to identify appropriate model. As one possible example, we performed subclassification of our models based on the expression of PARP, HDAC, SHH, and WNT, of which small molecule inhibitors are actively evaluated in medulloblastomas, and identified the xenograft models that can potentially be used for rationally designed preclinical drug screenings.

Discussion

A major assumption of using animal models for cancer research is that these models replicate the biology of their primary tumors.[9,10,12] In our study, we demonstrated that the primary tumor-based orthotopic xenograft mouse models of medulloblastoma were molecularly faithful to the original patients' tumors. They replicated the molecular characteristics of the original patients' tumors, and serial in vivo subtransplantation up to 5 times did not cause significant changes of gene expression profiles. Detailed data analysis identified all the dysregulated genes in each of the xenograft mouse models and demonstrated that different molecular subgroups of medulloblastoma, including the 4 subgroups (SHH, WNT, group C, and group D) that were most recently identified,[17] were represented in our model system at least twice. These 11 patient-specific xenograft mouse models have thus provided us with a unique and resourceful platform for biological studies and rationally designed preclinical drug screenings of childhood medulloblastoma.

Although it has long been recognized that the heterotransplantation of human tumor cells can cause genetic changes, the magnitude of molecular alterations has not been systematically evaluated. In this study, we showed that genetic drift does occur during the establishment of orthotopic xenograft mouse models established from primary patients' tumors, which represents an inevitable disadvantage associated with xenograft mouse models. Our finding that most of the genetic drift occurred during the transition from the patients' tumor to the first generation of xenograft tumors suggests that the initial change of microenvironment played a major role in causing genetic drift. Our identification of only 69 genes (at FDR = 0.001) involved in this panel of xenograft model provided much needed evidence to demonstrate that the overall impact of such genetic drift was minimal. In addition, our previous studies have shown that the xenograft blood vessels were derived from the mouse cells.[9] Because the gene chips used in this study are human specific, cDNA from mouse RNA did not hybridize to the probes of the chip. Therefore, the replacement of nontumor human cells, such as endothelial cells, with pericyted, inflammatory cells by the host (mouse) cells could have been one of the possible reasons for the initial changes in gene expression. Of note, the relative tumor take-rate of anaplastic medulloblastoma is higher than those of the classic and nodular subtypes. Although this may reflect the aggressive nature of the anaplastic medulloblastomas, it is still possible that the selection bias may also play a role.

Because of the limited availability and uncertainty of tumorigenicity of patients' tumor tissues, it is often difficult to establish a large cohort of animal models for immediate use of biological and/or preclinical drug screening. Serial subtransplantation has thus offered an important approach to expand the cohorts of an animal model. In fact, our previous studies have shown that tumor cells harvested from 1 intracerebellar xenograft would be enough for 200–2000 subtransplantations.[9] In this study, we further showed that only limited numbers of genes were altered during serial in vivo subtransplantation, indicating that the selective and/or adaptive pressures during the transition from human brain to mouse brain were not severe enough to cause major genetic changes in the engrafted medulloblastoma cells. Our data have thus provided experimental evidence to suggest that large cohorts of animal models can be safely expanded through subtransplantations to meet the needs of biological and preclinical studies for at least 5 passages.

Optimal use of xenograft models for drug testing also requires that xenograft models carry the molecular abnormalities that are designed for the target. Identification of molecularly appropriate xenograft models for specific inhibitor(s) or the models representing the molecular subtypes[17] is likely to have the most immediate preclinical usefulness. For example, our

identification of medulloblastoma models that carry activated SHH ($n = 2$) and WNT ($n = 2$) pathways, the 2 most common subtypes that were identified in all 3 previous studies,[15–17] makes it possible for a customized preclinical study to objectively evaluate the therapeutic efficacies of novel inhibitors targeting SHH or WNT. Our database containing all the differentially expressed genes/signaling pathways should therefore serve as a resourceful platform from which animal models with or without the intended molecular target(s) can be selected to examine the on-target and off-target efficacy of new therapies. The database will be of paramount importance in the future when comparing the changes of genomics profiles of different models in novel drug discovery processes.

In conclusion, we completed the first systematic molecular evaluation of a large panel of primary tumor-based orthotopic xenograft mouse models through global gene expression profiling. Our results demonstrated that these models are molecularly faithful, retaining most of the genetic abnormalities found in the original patients, and serial subtransplantation up to 5 passages only caused minor genetic drifts in the xenograft tumors. Using the recently identified molecular classifiers, we identified at least 2 models of each of the 4 molecular subtypes. This set of patient-specific and molecularly distinct xenograft mouse models should facilitate the comprehensive biological study and preclinical drug screenings for medulloblastoma. Our results provided strong molecular evidence to support the establishment and use of primary tumor-based orthotopic xenograft mouse models for human cancers.

Supplementary Material

Supplementary material is available at *Neuro-Oncology Journal* online (http://neuro-oncology.oxfordjournals.org/).

Funding

This work was funded by Cancer Fighters of Houston (X.N. Li).

Conflict of interest statement. None declared.

References

1. Strother D, Ashley D, Kellie SJ, et al. Feasibility of four consecutive high-dose chemotherapy cycles with stem-cell rescue for patients with newly diagnosed medulloblastoma or supratentorial primitive neuroectodermal tumor after craniospinal radiotherapy: results of a collaborative study. *J Clin Oncol*. 2001;19:2696–2704.
2. Taylor RE, Bailey CC, Robinson K, et al. Results of a randomized study of preradiation chemotherapy versus radiotherapy alone for nonmetastatic medulloblastoma: The International Society of Paediatric Oncology/United Kingdom Children's Cancer Study Group PNET-3 Study. *J Clin Oncol*. 2003;21:1581–1591.
3. Taylor RE, Bailey CC, Robinson KJ, et al. Outcome for patients with metastatic (M2–3) medulloblastoma treated with SIOP/UKCCSG PNET-3 chemotherapy. *Eur J Cancer*. 2005;41:727–734.
4. Dunkel IJ, Gardner SL, Garvin JH, Jr, Goldman S, Shi W, Finlay JL. High-dose carboplatin, thiotepa, and etoposide with autologous stem cell rescue for patients with previously irradiated recurrent medulloblastoma. *Neuro Oncol*. 2010;12:297–303.
5. Gajjar A, Pizer B. Role of high-dose chemotherapy for recurrent medulloblastoma and other CNS primitive neuroectodermal tumors. *Pediatr Blood Cancer*. 2010;54:649–651.
6. Gutmann DH, Maher EA, Van Dyke T. Mouse models of human cancers consortium workshop on nervous system tumors. *Cancer Res*. 2006;66:10–13.
7. Hoffman RM. Orthotopic metastatic (MetaMouse) models for discovery and development of novel chemotherapy. *Methods Mol Med*. 2005;111:297–322.
8. Shu Q, Antalffy B, Su JM, et al. Valproic Acid prolongs survival time of severe combined immunodeficient mice bearing intracerebellar orthotopic medulloblastoma xenografts. *Clin Cancer Res*. 2006;12:4687–4694.
9. Shu Q, Wong KK, Su JM, et al. Direct orthotopic transplantation of fresh surgical specimen preserves CD133+ tumor cells in clinically relevant mouse models of medulloblastoma and glioma. *Stem Cells*. 2008;26:1414–1424.
10. Yu L, Baxter PA, Voicu H, et al. A clinically relevant orthotopic xenograft model of ependymoma that maintains the genomic signature of the primary tumor and preserves cancer stem cells in vivo. *Neuro Oncol*. 2010;12:580–594.
11. Hoffman RM. Orthotopic metastatic mouse models for anticancer drug discovery and evaluation: a bridge to the clinic. *Invest New Drugs*. 1999;17:343–359.
12. Whiteford CC, Bilke S, Greer BT, et al. Credentialing preclinical pediatric xenograft models using gene expression and tissue microarray analysis. *Cancer Res*. 2007;67:32–40.
13. Gilbertson RJ. Medulloblastoma: signalling a change in treatment. *Lancet Oncol*. 2004;5:209–218.
14. Packer RJ. Risk stratification of medulloblastoma: a paradigm for future childhood brain tumor management strategies. *Curr Neurol Neurosci Rep*. 2011;11:124–126.
15. Thompson MC, Fuller C, Hogg TL, et al. Genomics identifies medulloblastoma subgroups that are enriched for specific genetic alterations. *J Clin Oncol*. 2006;24:1924–1931.
16. Kool M, Koster J, Bunt J, et al. Integrated genomics identifies five medulloblastoma subtypes with distinct genetic profiles, pathway signatures and clinicopathological features. *PLoS ONE*. 2008;3:e3088.
17. Northcott PA, Korshunov A, Witt H, et al. Medulloblastoma Comprises Four Distinct Molecular Variants. *J Clin Oncol*. 2010;14:1408–1414.
18. Anderton JA, Lindsey JC, Lusher ME, et al. Global analysis of the medulloblastoma epigenome identifies disease-subgroup-specific inactivation of COL1A2. *Neuro Oncol*. 2008;10:981–994.

19. Schwalbe EC, Lindsey JC, Straughton D, et al. Rapid diagnosis of medulloblastoma molecular subgroups. *Clin Cancer Res*. 2011;17:1883–1894.
20. Ellison DW, Dalton J, Kocak M, et al. Medulloblastoma: clinicopathological correlates of SHH, WNT, and non-SHH/WNT molecular subgroups. *Acta Neuropathol*. 2011;121: 381–396.
21. Cho YJ, Tsherniak A, Tamayo P, et al. Integrative genomic analysis of medulloblastoma identifies a molecular subgroup that drives poor clinical outcome. *J Clin Oncol*. 2011;29:1424–1430.
22. Li XN, Shu Q, Su JM, Perlaky L, Blaney SM, Lau CC. Valproic acid induces growth arrest, apoptosis, and senescence in medulloblastomas by increasing histone hyperacetylation and regulating expression of p21Cip1, CDK4, and CMYC. *Mol Cancer Ther*. 2005;4:1912–1922.
23. Li XN, Parikh S, Shu Q, et al. Phenylbutyrate and phenylacetate induce differentiation and inhibit proliferation of human medulloblastoma cells. *Clin Cancer Res*. 2004;10:1150–1159.
24. Tusher VG, Tibshirani R, Chu G. Significance analysis of microarrays applied to the ionizing radiation response. *Proc Natl Acad Sci USA*. 2001;98:5116–5121.